B 8.1

PIEZOELECTRIC TRANSFORMER OF TRAVELLING WAVE TYPE

C. Kauczor[1], T. Schulte[3], H. Grotstollen[2]

[1]Heinz Nixdorf Institute, Mechatronics and Dynamics, University of Paderborn, Germany
[2]Institute for Power Electronics and Electrical Drives, University of Paderborn, Germany
[3]was with the above institute until April 2003

Abstract:
Various designs of piezoelectric transformers are known, but due to the limitation of a finite mechanical structure only standing wave excitation is used up to now. This paper outlines a novel concept based on a travelling wave instead of standing wave excitation, which allows a theoretical increase of power density by a factor of $\sqrt{2}$. The theoretical basics as well as measurements on a prototype of a travelling wave type piezoelectric transformer are presented.

Keywords: piezoelectric transformer, travelling wave, switched mode power supplies

Introduction

Switched mode power supplies are mainly equipped with electromagnetic transformers but the progress in miniaturisation of those components is slowing down. An alternative is the utilisation of piezoelectric transformers (PT) in switched mode power supplies for small output power. The energy transfer is realised by the piezoelectric effect: A mechanical oscillation excited on the primary side is reconverted into electrical signals on the secondary side of the piezoelectric device. Typical characteristics of piezoelectric transformers are e. g. high power density and high insulation capability, which qualify them for portable devices as laptops and mobile phones. A well-known application is the back-light system with cold cathode fluorescent lamps for LCD-displays. Typical are these types of piezoelectric transformers, based on the so called Rosen-transformer [1]. Newer concepts use multi-layer techniques to exploit the power capability at lower voltages [2]. Various designs are known, but due to the limitation of a finite mechanical structure, only standing wave excitation is used up to now. In these configurations a considerable part of the material acts mainly passive as bulk and can not be used to inject or extract energy.
This contribution presents a novel concept based on a travelling wave instead of standing wave excitation. In order to generate a travelling wave a multi-phase system (minimum two phases) for primary and secondary side is of course required.

The Idea of a Piezoelectric Transformer of Travelling Wave Type (TWPT)

For outlining the idea an infinite beam is considered which has an electrode configuration building segments of length L. The even numbered segments and the odd numbered segments build two orthogonal oscillation systems (index 1 and 2). When a system is excited by a sinusoidal voltage $v_{1,2}(t)$ of appropriate frequency a standing displacement wave $u_{1,2}(x,t)$ with wave length $4L$ is generated. Superimposing the two orthogonal standing waves with equal amplitudes a pure standing wave is generated, if the phase shift is 0° and a pure travelling wave, if the phase shift is ±90°, see Fig. 1.

$$\hat{u}_1(x,t) = \hat{u}_1 \cos\left(x \cdot L/\lambda\right) \cdot \sin(\omega \cdot t + \varphi_1)$$
$$\hat{u}_2(x,t) = \hat{u}_2 \sin\left(x \cdot L/\lambda\right) \cdot \sin(\omega \cdot t + \varphi_2)$$
$$\text{standing wave}: \varphi_2 - \varphi_2 = 0,\ \hat{u}_1 = \hat{u}_2$$
$$\text{travelling wave}: \varphi_2 - \varphi_2 = \pi/2,\ \hat{u}_1 = \hat{u}_2$$

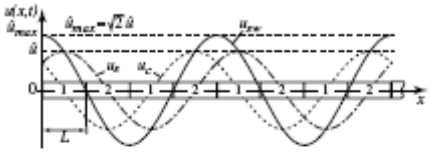

Fig. 1: Superimposed oscillation modes.

In case of a pure standing wave the maximum amplitude $\hat{U}$ of the displacement is $\sqrt{2}$ -times higher than in the case of travelling wave operation. In a piezoelectric transformer the transferable energy is limited by the maximum permissible mechanical tensile stress $\hat{T}_{max.}$ without damaging the ceramic material and the maximum permissible electrode voltage. Beyond this voltage depolarisation effects occur. Operation with voltages far below this limit reduces significantly the power density of the transformer.
Considering the maximum mechanical stress the utilisation of the material is higher, when a travelling wave is excited, since the amplitudes $\hat{u}_{1,2}$ of the orthogonal standing wave can be higher. In order to estimate the

$$\hat{S}^i(x) = \frac{\partial}{\partial x}\hat{U}^i(x)\,. \qquad (6)$$

The amplitude of the stress $\hat{T}^i(x)$ is calculated by the constitutive piezoelectric law

$$\hat{T}^i(x) = \frac{1}{s^E}\hat{S}^i(x) - \frac{d}{s^E}\hat{E}^i = c^E\hat{S}^i(x) - e\hat{E}^i\,, \quad (7)$$

and using Eq. (6) results in ($\hat{E}^i = \hat{V}^i/a$)

$$\hat{T}^i(x) = c^E\frac{\partial}{\partial x}\hat{U}^i(x) - \frac{e}{a}\hat{V}^i\,. \qquad (8)$$

Continous conditions for displacement $u(x,t)$ and stress $T(x,t)$ must be fulfilled at the boundaries of each segment (area i and $i+1$), where are the contact areas to the next segment (9)

$$\hat{U}^i\left(\frac{L}{2}\right) = \hat{U}^{i+1}\left(-\frac{L}{2}\right),\quad \hat{T}^i\left(\frac{L}{2}\right) = \hat{T}^{i+1}\left(-\frac{L}{2}\right)\quad n = 1..3$$

$$\hat{U}^4\left(\frac{L}{2}\right) = \hat{U}^1\left(-\frac{L}{2}\right),\quad \hat{T}^4\left(\frac{L}{2}\right) = \hat{T}^1\left(-\frac{L}{2}\right)\quad n = 4$$

Using all boundary conditions of Eq. (9) yields a linear system of equations with the vector $\vec{r}$ containing the boundary conditions and the vector $\vec{k}$ with the constants $\hat{U}_f^i$, $\hat{U}_r^i$ in all four segments:

$$\vec{r} = \mathbf{M}\cdot\vec{k} \qquad (10)$$

with

$$\mathbf{M} = \begin{bmatrix} \mathbf{m}_1 & \mathbf{m}_2 \\ \mathbf{m}_1 & -\mathbf{m}_2 \end{bmatrix},\quad \vec{r} = \begin{bmatrix} 0 & 0 & 0 & 0 & \tau^1 & \tau^2 & \tau^3 & \tau^4 \end{bmatrix}^T$$

$$\vec{k} = \begin{bmatrix} \hat{U}_f^1 & \hat{U}_f^2 & \hat{U}_f^3 & \hat{U}_f^4 & \hat{U}_r^1 & \hat{U}_r^2 & \hat{U}_r^3 & \hat{U}_r^4 \end{bmatrix}^T$$

and

$$\mathbf{m}_1 = \begin{bmatrix} e^{-j\frac{\omega L}{c\,2}} & 0 & 0 & -e^{j\frac{\omega L}{c\,2}} \\ -e^{j\frac{\omega L}{c\,2}} & e^{-j\frac{\omega L}{c\,2}} & 0 & 0 \\ 0 & -e^{j\frac{\omega L}{c\,2}} & e^{-j\frac{\omega L}{c\,2}} & 0 \\ 0 & 0 & -e^{j\frac{\omega L}{c\,2}} & e^{-j\frac{\omega L}{c\,2}} \end{bmatrix},$$

$$\mathbf{m}_2 = \begin{bmatrix} e^{j\frac{\omega L}{c\,2}} & 0 & 0 & -e^{-j\frac{\omega L}{c\,2}} \\ -e^{-j\frac{\omega L}{c\,2}} & e^{j\frac{\omega L}{c\,2}} & 0 & 0 \\ 0 & -e^{-j\frac{\omega L}{c\,2}} & e^{j\frac{\omega L}{c\,2}} & 0 \\ 0 & 0 & -e^{-j\frac{\omega L}{c\,2}} & e^{j\frac{\omega L}{c\,2}} \end{bmatrix}.$$

Constants τ^i are defined as

$$\tau^i = \frac{-j\cdot c}{c^E\omega}\cdot\frac{e}{a}\cdot(\hat{V}^{i+1} - \hat{V}^i)\,. \qquad (11)$$

The current is obtained solving the surface integral of the electric displacement and differentiation with respect to time (ε^T: permittivity of the material):

$$\hat{D}^i(x) = d\hat{T}^i(x) + \varepsilon^T\frac{\hat{V}^i}{a} \qquad (12)$$

$$\Rightarrow\ \hat{I}^i = \oint_{A_{electrode}}\frac{\partial\hat{D}^i(x)}{\partial t} = j\omega\cdot b\cdot\int_{-L/2}^{L/2}\hat{D}^i(x)\cdot dx \qquad (13)$$

The calculation of the current $\hat{I}^1$ of the analysed structure is now given by $\vec{Y} = b\cdot d\cdot e\cdot c\,l/(2a)$. The constant C is a capacitance calculated from geometric and material parameters

$$C = L\cdot b\cdot(d\cdot e - \varepsilon^T)/a\,. \qquad (14)$$

$$\Rightarrow \hat{I}^1 = j\left(-\omega C + K\left(\tan\left(\frac{\omega L}{c\,2}\right) + \tan\left(\frac{\omega}{c}L\right)\right)\hat{v}_1 - \right.$$

$$\left. - jc\tan\left(\frac{\omega L}{c\,2}\right)(\hat{v}_2 + \hat{v}_4) + jc\left(\tan\left(\frac{\omega L}{c\,2}\right) - \tan\left(\frac{\omega}{c}L\right)\right)\hat{v}_3$$

In case of operation close to resonance frequency $\omega \to \omega_0 = c\pi/(2L)$ all terms with $\tan(\omega L/(2c))$ are negligible compared to terms $\tan(\omega L/c)$ which become infinite for $\omega = \omega_0$. The resulting approximation of the admittance matrix reduces thus to

$$\begin{bmatrix} \hat{I}_1 \\ \hat{I}_2 \\ \hat{I}_3 \\ \hat{I}_4 \end{bmatrix} = \begin{bmatrix} -j\omega C & 0 & 0 & 0 \\ 0 & -j\omega C & 0 & 0 \\ 0 & 0 & -j\omega C & 0 \\ 0 & 0 & 0 & -j\omega C \end{bmatrix}\cdot\begin{bmatrix} \hat{V}_1 \\ \hat{V}_2 \\ \hat{V}_3 \\ \hat{V}_4 \end{bmatrix} +$$

$$+\vec{Y}\cdot\begin{bmatrix} 1 & 0 & -1 & 0 \\ 0 & 1 & 0 & -1 \\ -1 & 0 & 1 & 0 \\ 0 & -1 & 0 & 1 \end{bmatrix}\cdot\begin{bmatrix} \hat{V}_1 \\ \hat{V}_2 \\ \hat{V}_3 \\ \hat{V}_4 \end{bmatrix}$$

$$\mathbf{I} = \mathbf{C}\cdot\mathbf{V} + \vec{Y}\cdot\mathbf{K}\cdot\mathbf{V} \qquad (15)$$

Matrix **K** points out the coupling between the segment with index 1 and 3 as well as between segment 2 and 4. Each pair 1 and 3 as well as 2 and 4 build one phase of the TWPT with almost no cross coupling between the phases. If one segment (e. g. index 1) acts as an input (primary side) and the other (index 3) acts as an output (secondary side), a phase shift of 180° between input and output signal results. Capacitance matrix **C** represents the dielectric part of the electrical system (piezoelectric capacitance).

Possible Structures of TWPT and Realisation

As a crossover from an infinite structure, discussed in the previous section, to a realisable system the use of a rotation-symmetrical structure is one possible solution. Therefore all ring-, disc- or tube-shaped configurations are potential candidates for implementation. As a first approach a ring-shaped 2λ-wave length oscillator with eight separate excitation segments was realised for testing purposes, see Fig. 6.

Four segments (two for primary and two for secondary side) are used for the energy transfer within one independent phase. The two groups of four segments correspond to two orthogonal standing waves, which are superimposed to generate the travelling wave. The data of the prototype is listed in Table 1.

increase of power density the equ
cuit of the PT shown in Fig. 2 is co

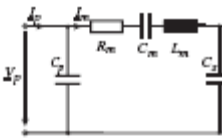

Fig. 2: Equivalent circu

It is assumed, that the input is cha
mum permissible voltage and the
adjusted for having the maximu
chanical stress. Considering r
($\omega = 1/\sqrt{L_m C_m}$) and neglecting
sumed to equal $\hat{V}_p$.

Neglecting the influence of the elec
the constitutive equations (co
$\hat{T} \propto \hat{U}$ can be stated as an approp
in case of resonant operation where
maximum stress value. Introducing
above, in case of travelling wave c
tudes $\hat{u}_{1,2}$ of the orthogonal stand
$\sqrt{2}$-times higher without exceeding
sible stress $\hat{T}_{max}$. Since $\hat{U}_{1,2} \propto$
$\hat{I}_m$ can be $\sqrt{2}$-times higher. As
diagram of Fig. 3 the increase of t
least higher by a factor $\sqrt{2}$. The
transferred power in both op
$P_L^{SW} = \hat{I}_L\hat{V}_s\cdot 1/2$ for standi
$P_L^{TW} = \hat{I}_L\hat{V}_s/(2\sqrt{2})$ for travelling w

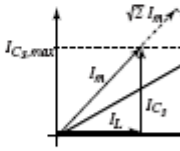

Fig. 3: Currents at travelling w

Calculation of characteristic pa

In this section the calculation
modes in the above-explained sy
at a continuum-mechanical systen
equations the superscript i indica
of the structure.

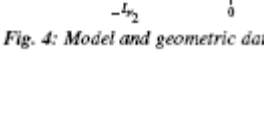

Fig. 4: Model and geometric da

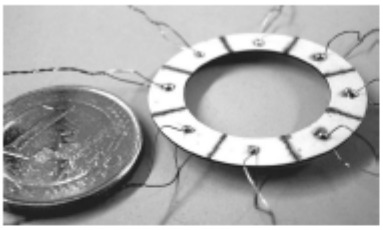

Fig. 6: Realised TWPT.

Inner diameter R_i	10 mm
Outer diameter R_o	15 mm
Thickness a	0,5 mm
Density ρ	7,85 g/cm^3
Elastic constant c_{11}^E	$1/11{,}8 \cdot 10^{-12}$ N/m^2
f_2 ($2c/A$; A=2 π 12,5 mm)	83,669 kHz

Table 1: Characteristic values of the realised TWPT.

First the voltage transfer behaviour was measured in order to find the exact resonance frequencies of both oscillation systems. The voltage ratio of input and output is plotted for frequencies between 10 kHz and 200 kHz in Fig. 7.

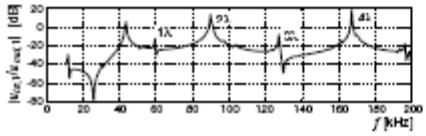

Fig. 7: Voltage transfer behaviour of the realised TWPT.

The oscillation mode of interest (2λ-mode) has a frequency of about 90 kHz, which equals almost the calculated frequency. Small differences can be traced back to the ring-shape, which is not considered in the calculation (Table 1). A closer look at both oscillation systems is shown in Fig. 8.

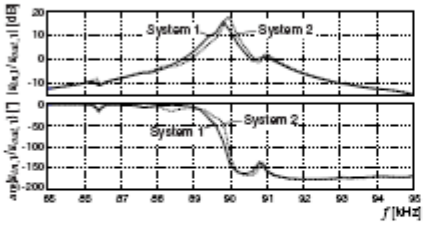

Fig. 8: Voltage transfer behaviour of the realised TWPT at 2λ-mode.

FEM Simulation and Development Potential

Since all segments have a similar electrode configuration, the transfer ratio between primary and secondary side is 1 (not considering the resonant gain). Moreover the result of a FEM simulation (Fig. 9) shows that the displacement is a function of the radius. Therefore the assumption of consistent conditions within the cross section as for the infinite beam are not fulfilled. The utilisation of the piezoceramic is poor at the inner rim of the ring.

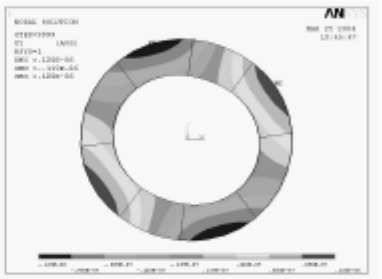

Fig. 9: Mechanical Displacement calculation by FEM Simulation of a ring-shaped TWPT.

For exploiting the theoretical increase in power density (factor $\sqrt{2}$) a more efficient implementation is to be found, also incorporating a transfer ratio $\neq 1$.
This should be feasible by use of ring-shaped structures operated at $n\lambda$-mode with $n >> 2$ and multilayer technique. A drawback will be the connection problem due to the high amount of separate electrodes.

Conclusions

In this paper a novel concept for piezoelectric transformers is presented, using travelling waves instead of standing waves to increase the power density of the piezoelectric ceramic. The theoretical basics as well as measurements and simulations of a finite element model of a realised prototype is presented.

References

[1] Charles A. Rosen et al.: Electromechanical Transducer, US-Patent 2,830,274, 1958

[2] J. Navas, T. Bove et al.: Miniaturised Battery Charger using Piezoelectric Transformers, APEC 2001, Los Angeles, March 2001

[3] T. Hemsel, W. Littmann, J. Wallaschek: Piezoelectric Transformers – State of the Art and Development Trends, IEEE Ultrasonics Symposium Munich, October 2002 (2003)